In-plane buckling of beech LVL columns

Janusch Töpler, Institute of Structural Design, University of Stuttgart, Germany

Ulrike Kuhlmann, Institute of Structural Design, University of Stuttgart, Germany

Keywords: Stability, in-plane buckling, beech LVL, imperfections, experimental results, numerical modelling, Finite Element based design, effective length method

1 Introduction

Glulam made of beech laminated veneer lumber (beech LVL) is increasingly used in timber construction, due to improved availability and high strengths and stiffnesses, especially for columns in multi-storey buildings and high-rise buildings.

Beech LVL columns in building practice are usually at risk of in-plane buckling and can currently be designed according to EN 1995-1-1 (2004) with the equivalent length method (ELM; EC5, section 6.3.2) or interaction equations with calculation of internal forces according to second order theory (T2O; EC5, section 6.2.4). These design methods were developed for softwood columns (EHLBECK & BLAß (1987)). A validation of these design methods for beech LVL by means of experimental investigations has not yet been carried out. Differences between design of softwood and hardwood column are to be expected, since on the one hand the stress-strain relationships of the materials parallel to the grain differ significantly (EHRHART ET AL. (2021 b)), and on the other hand the production-related imperfections (bow) may be different.

Figure 1.1. Buckling test of a beech LVL column with length x width x height = 2500 x 200 x 200 mm.

Within the Cluster of Excellence *Integrative Computational Design in Architecture and Construction* (IntCDC) (KUHLMANN ET AL. (2022)) 27 buckling tests on beech LVL columns were carried out by the Institute

of Structural Design at the MPA Stuttgart in spring 2022 (Figure 1.1), in order to determine the buckling behaviour of beech LVL columns.

This paper presents the experimental results of 27 buckling tests (Figure 1.1) and preceding tests for determination of the modulus of elasticity of each test specimen and the stress-strain curve of beech LVL under compression parallel to the grain. Subsequently, a numerical model was developed and validated using the experimental results. Based on numerical calculations with nominal values for geometry, material and bow imperfections the maximum load-bearing capacities for in-plane buckling of beech LVL columns were determined and a provisional safe-sided design proposal was developed. This derivation follows the design method *Numerical design with direct resistance check* as it is defined in TÖPLER ET AL. (2022) or prEN 1993-1-14 (2022). The findings are compared with literature and current design rules.

Incorporated in the investigations are results of the DIBt research project P 52-5-13.194-2048/19 (KUHLMANN & TÖPLER (2022 b)), where, among others, bow imperfections of beech LVL columns and beams were measured in newly erected buildings.

This paper is intended to form a basis for the derivation of the in-plane buckling verification of beech LVL columns.

2 State of the art

EN 1995-1-1 (2004) gives two design approaches for slender timber columns, the effective length method (ELM) and design verification based on calculation of internal forces according to second order theory (T2O).

In ELM the compression strength is reduced by the factor k_c, accounting for second order effects (geometrically nonlinear behaviour) and to a certain extend also for materially nonlinear behaviour. The formulas for determination of k_c in EN 1995-1-1 (2004) can be derived directly from the verification according to T2O assuming a linear interaction of axial force and bending moment as demonstrated by SCHÄNZLIN (2022). It is necessary to consider that the compressive strength parallel to the grain $f_{c,0,k}$ was determined on test specimen with a relative slenderness ratio $\lambda_{rel} = 0.3$. Therefore, a reduction of the relative slenderness ($\lambda_{rel} - 0.3$) is applied. k_c depends on the β_c factor which covers the effects of bow imperfections and the ratio of $E_{0,05} : f_{c,0,k} : f_{m,k}$. β_c may also be used accounting for plasticizing in compression parallel to the grain. $\lambda_{rel,0}$ and β_c were defined based on the numerical investigations by EHLBECK & BLAß (1987) on softwood columns made of glulam (grade I and II, DIN 4074 (1958)) and solid timber (grade II) including stochastic material modelling and measured geometrical imperfections. For softwood columns made of glulam $\beta_c = 0.1$ (≙ bow imperfection of $e_y \approx L/1100$) and for solid timber $\beta_c = 0.2$ (≙ bow imperfection of $e_y \approx L/470$) were determined.
Effects of load eccentricities and sway imperfections (e.g. for design of cantilever columns, see SCHÄNZLIN (2022)) should be considered separately.

When internal forces are determined using T2O, the interaction formula for verification according EN 1995-1-1 (2004) includes a squaring of the axial force component, which was derived empirically based on the investigations of BUCHANAN ET AL. (1985). The equivalent bow imperfections given in EN 1995-1-1 (2004) for T2O (e_y = L/400) are not the same as assumed within ELM, but on the safe side.

For columns made of spruce glulam GL 24h and GL 32h FRANGI ET AL. (2015) and for beech glulam GL 40h, GL 48h and GL 55h EHRHART ET AL. (2019) experimentally and numerically determined lower load-bearing capacities (up to 18 %) than those obtained by ELM with β_c = 0.1 according to EN 1995-1-1(2004). This is partly due to the larger assumed imperfections (e_y = L/380 to L/570) and partly because of a different ratio of $E_{0,05} : f_{c,0,k} : f_{m,k}$ for beech glulam.

In the current revision process of Eurocode 5 (prEN 1995-1-1 (2021)) the mentioned parts and formulas of ELM and T2O for in-plane buckling are kept largely unchanged, but issues of the application limits of ELM and the named inconsistencies of imperfection assumptions are discussed.

3 Experiments

3.1 General

Buckling tests on 27 beech LVL columns made of GL75 according to ETA-14/0354 (2018) were conducted in order to experimentally determine the buckling behaviour and serve as validation for a FE model, which is subsequently used to assess the characteristic buckling resistance. Additional relevant input values for the FE model are the modulus of elasticity and the stress-strain curve for compression parallel to the grain, which were determined in preceding tests. The test specimens were wrapped in vapour-proof foil during the test period to prevent changes in the wood moisture content. The test specimens are given in Table 3.1.

Table 3.1. Beech LVL GL75 test specimens for buckling and preceding elastic 4-point bending tests

Series number	Number of specimens	Length [mm]	Width x Height [mm²]	λ_{rel} [1]	Orientation of lamellae	Load eccentricity
S01 - S03	3	3000	120 x 120	1.88	flatwise	Width / 10
S04 - S06	3	3000	160 x 160	1.41	flatwise	Width / 10
S07 - S09	3	3000	200 x 200	1.13	flatwise	Width / 10
S10 - S12	3	2500	200 x 200	0.94	flatwise	Width / 6.7
S13 - S15	3	2500	200 x 200	0.94	edgewise	Width / 10
S16 - S18	3	2500	200 x 200	0.94	flatwise	Width / 10
S19 - S21	3	2500	200 x 200	0.94	flatwise	Width / 20
S22 - S24	3	2000	200 x 200	0.75	flatwise	Width / 10
S25 - S27	3	2000	200 x 200	0.75	edgewise	Width / 10

[1] Calculated with $E_{0,05}$ = 16469 N/mm² and $f_{c,0}$ = 76.9 N/mm²

3.2 Preceding elastic 4-point bending tests

For each column test specimen one elastic 4-point bending test according to EN 408 (2010) was conducted to determine the bending modulus of elasticity $E_{L,m}$ (Figure 3.1). The orientation of the lamellae was chosen along the column tests (Table 3.1).

The results are summarized in Table 3.2. $E_{L,m}$ is in good agreement with previous test results (KUHLMANN & TÖPLER (2022 a)) and literature (e.g. EHRHART ET AL. (2021 a)), indicating a low wood moisture content (approximately 6 to 7 %).

Table 3.2. Results of elastic 4-point bending tests on beech LVL GL75

	Mean	COV
Modulus of elasticity $E_{L,m}$ [N/mm²]	16469	0.048
Density ρ [kg/m³]	803	0.011

3.3 Preceding compression tests parallel to the grain

Five compression tests parallel to the grain according to EN 408 (2010) were conducted to determine the compression strength $f_{c,0}$ and the stress-strain curve of beech LVL GL75 (Figure 3.2). The dimensions were chosen to length x height x width = 300 x 120 x 50 mm³ to correspond with compression tests for determination of the compressive strength $f_{c,0,k}$ of GL75 carried out by DILL-LANGER (2014). The ratio height / width = 6 also defines $\lambda_{rel,0}$. The orientation of the lamellae was parallel to the short side (width).

The vertical deformations were measured with two displacement transducers at both sides of the test specimens over a length of 230 mm (Figure 3.2).

Exemplary, Figure 3.3 shows the axial force-deformation curve of test specimen 2_1. On the horizontal axis the mean of both displacement transducers is displayed. The vertical axis exhibits the machine force. The curve is linear elastic up to approx. 65 %

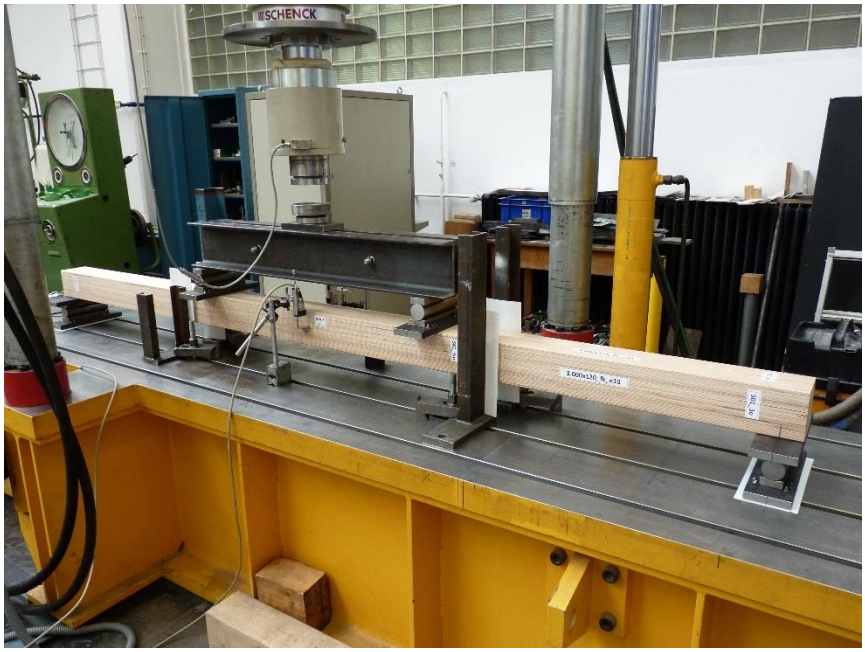

Figure 3.1. Elastic 4-point bending test with length x width x height = 2500 x 200 x 200 mm³.

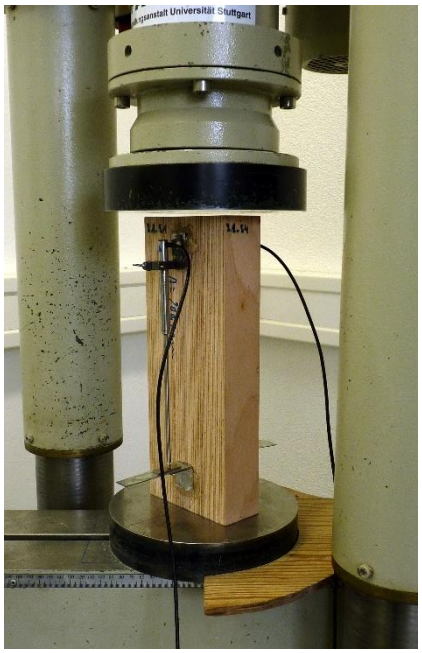

Figure 3.2. Compression test parallel to the grain.

of F_{max}. Subsequently, a considerable plasticising occurs until the compressive strength $f_{c,0,2}$ is reached, followed by a drop in load. During plasticising, a visible buckling of the fibres occurred at the corners of the test specimen and, after reaching the compressive strength, the fibre buckling (partly in the form of a kink band with an inclination of approx. 45 °) spread over the entire cross-section. In the evaluation, the beginning of plasticising / proportionality limit $f_{c,0,1}$ (Figure 3.3, point 1) is defined as the point, at which the total strains ε_{el+pl} exceed the linear elastic strains $\varepsilon_{el} = \sigma / E_{c,0}$ by 5 %. The mean results of the tests are summarized in Table 3.3.

Table 3.3. Results of 5 compression tests parallel to the grain on beech LVL GL75

	Mean	COV
Compression strength $f_{c,0,2}$ [N/mm²]	76.9	0.038
Proportionality limit $f_{c,0,1}$ [N/mm²]	48.1	0.189
Plastic strain $\varepsilon_{pl,0,2}$ when reaching $f_{c,0,2}$ [-]	1.26 x $\varepsilon_{el,0,2}$	0.188
Modulus of elasticity $E_{c,0}$ [N/mm²]	16216	0.030
Density ρ [kg/m³]	798	0.004

The scatter of $f_{c,0,2}$ and the $E_{c,0}$ is very low, which is due to the fact that all test specimens were fabricated from the same residual piece of a column test specimen and that the material was very homogeneous.

The large plastic strains of beech LVL are remarkable (Table 3.3). For softwood, $\varepsilon_{pl,0,2} = 0.25$ x $\varepsilon_{el,0,2}$ according to GLOS (1978) is usually assumed. For beech LVL the experimentally determined plastic strains $\varepsilon_{pl,0,2}$ are 4 to 6.5 times higher.

Fortunately, the experimental data of EHRHART ET AL. (2021 b) could be evaluated to validate the own results. These values are presented in Table 3.4. This evaluation of the strains was based on the cylinder displacement and is therefore subject to some uncertainty. The plastic strain was determined to $\varepsilon_{pl,0,2} \approx 1.5$ x $\varepsilon_{el,0,2}$ and the proportionality limit to $f_{c,0,1} \approx 0.75$ x $f_{c,0,2}$. For high moisture contents (u = 16.9 %, service class (SC) 2) smaller plastic strains $\varepsilon_{pl,0,2} \approx 1.15$ x $\varepsilon_{el,0,2}$ were observed.

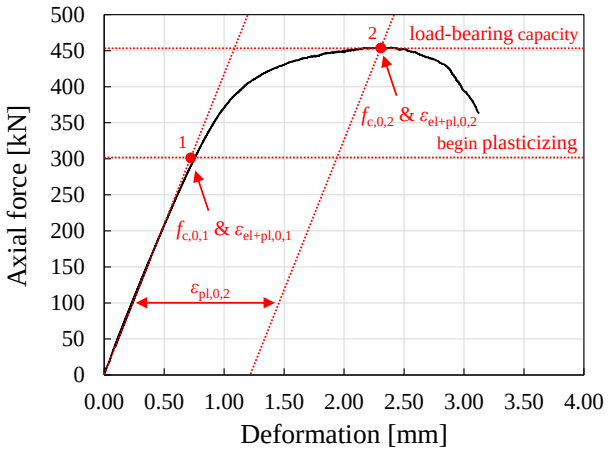

Figure 3.3. Axial force-deformation curve of compression test 2_1, including important points for derivation of stress-strain curve.

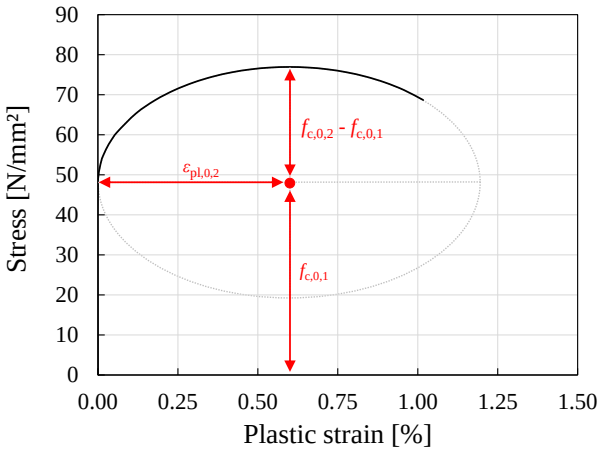

Figure 3.4. Mean stress-plastic strain curve mapped by an ellipse with radii $\varepsilon_{pl,0,2}$ and ($f_{c,0,2}$ - $f_{c,0,1}$), values derived from the compression tests.

Table 3.4. Evaluation of the stress-strain curves of compression tests parallel to the grain on beech LVL by EHRHART ET AL. (2021 b), mean values with (COV), 6 tests per moisture content

Moisture content [%]	$E_{c,0}$ [N/mm²]	$f_{c,0,2}$ [N/mm²]	$f_{c,0,1}$ [N/mm²]	$\varepsilon_{pl,0,2}$ [-]	*Ellipse for plasticising* $\varepsilon_{pl,0,2}$ [x $\varepsilon_{el,0,2}$]	*Ellipse for plasticising* $f_{c,0,2} - f_{c,0,1}$ [x $f_{c,0,2}$]
6.1	16156 (0.026)	80.4 (0.011)	59.3 (0.030)	0.0076 (0.116)	1.52 (0.103)	0.26 (0.058)
7.0	16052 (0.025)	73.1 (0.031)	56.1 (0.027)	0.0076 (0.133)	1.66 (0.118)	0.23 (0.062)
8.9	15828 (0.01)	64.0 (0.014)	49.8 (0.020)	0.0061 (0.068)	1.50 (0.054)	0.22 (0.082)
16.9	14815 (0.039)	39.1 (0.034)	29.4 (0.150)	0.0030 (0.064)	1.14 (0.061)	0.25 (0.379)

The plastic strains can be mapped by means of an ellipse (Figure 3.4) as proposed by GROSSE (2005), where ($f_{c,0,2}$ - $f_{c,0,1}$) and $\varepsilon_{pl,0,2}$ represent the ellipse radii. Numerical comparative calculations modelling plasticising with such an approach show good agreement with the experimental results.

Based on the results in Table 3.3 $\varepsilon_{pl,0,2}$ = 1.25 x $\varepsilon_{el,0,2}$ and $f_{c,0,1}$ = 0.65 x $f_{c,0,2}$ are chosen for further calculations.

3.4 Column tests

3.4.1 General

Buckling tests on 27 beech LVL columns made of beech LVL GL75 were conducted in a 15 MN testing facility at MPA Stuttgart in order to experimentally investigate the buckling behaviour and serve as validation for a FE model. The column dimensions (slenderness), load eccentricity and lamellae orientation were varied.

3.4.2 Test programme, setup and execution

The test specimens, dimensions, orientations of lamellae and load eccentricities are given in Table 3.1. The dimensions were chosen to represent typical values of medium slender columns in building practice. As the flatwise bending strength is expected to be lower, this orientation was chosen as default. To force an in-plane buckling in a defined direction, the axial load was applied eccentrically.

Tilting bearings were arranged at the column top and base in order to allow for an unrestricted rotation around one axis (Figure 1.1). The structural system thus corresponds to Euler buckling mode 2 with a minimal rotational spring at the supports. The rotation points of the tilting bearings had a distance of 153 mm and 154 mm to the column surface. The load eccentricity was realised via a similar offset of the columns at both tilting bearings. As protection when the columns fail, horizontal timber beams were arranged to prevent the test specimen from falling out of the test facility (Figure 1.1). Loading was applied displacement-controlled from the bottom at a speed of 2

mm/min. The first load cycle was conducted up to 80 kN and the second load cycle until failure of the column. The measurements were conducted with the optical measuring system ARAMIS Adjustable 12M, which very precisely determined the position of defined points in space in time steps (here every 10 s) by means of digital image correlation. For this purpose, a stochastic pattern was applied onto two sides of the test specimens at midspan (Figure 1.1). This was supplemented by measurement points attached to the supports. The measuring system was set up at a 45 ° angle to the sides of the columns in order to measure two sides in parallel (according to direction of view in Figure 1.1). Beforehand, the member dimensions and the weight were documented.

3.4.3 Results and evaluation

The horizontal and vertical deformations at midspan and at the supports and the rotations at the supports were analysed. The results of column S01 are not shown because there the bottom support was realised differently so that high friction occurred and the bearing acted as a restraint.

The horizontal deformations at midspan U_y and the corresponding axial forces F are exemplary displayed in Figure 3.5 for column S08. The curve is non-linear from the beginning. After the load-bearing capacity F_{max} was reached, the horizontal deformations U_y increased significantly with a moderate load drop until the brittle failure of the test specimen occurred. This behaviour was the same for all columns, with different maximum load-bearing capacities F_{max} (192 to 1634 kN) and maximum horizontal deformations U_y (60 to 190 mm).

The experimentally determined normalised load-bearing capacities k_c of all columns are plotted in Figure 3.6 over the relative slenderness ratio λ_{rel}. The data show a very low scatter and follow well the expected shape of a buckling curve. k_c and λ_{rel} are computed using the measured modulus of elasticity of each column and $f_{c,0}$ = 76.9 N/mm². N_{crit} is calculated with $E_{L,m}$ = 16469 N/mm² (Figure 3.2).

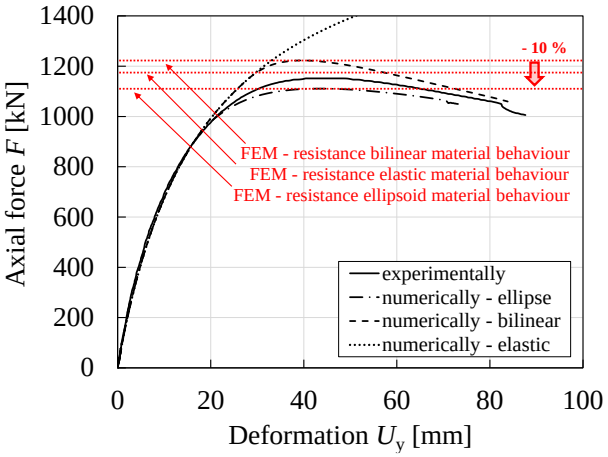

Figure 3.5. Axial force F and horizontal deformation U_y at midspan of column S08 with length x width x height = 2500 x 200 x 200 mm³, experimental and numerical results considering different material models.

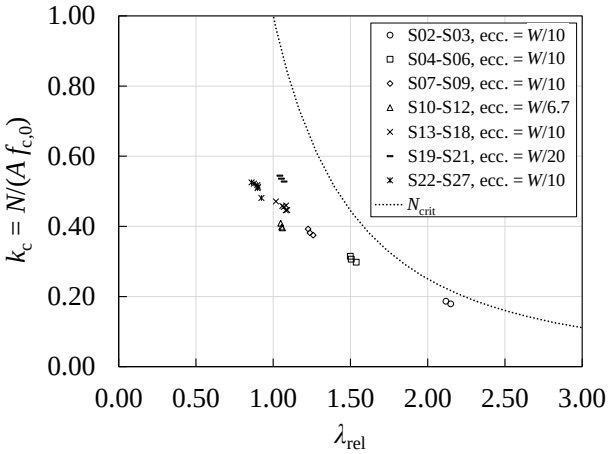

Figure 3.6. Experimentally determined, normalised load-bearing capacities k_c of columns S02 to S27 plotted over the slenderness ratio λ_{rel} with variing eccentricity depending on the width W.

Figure 3.7. Column S22 after failure; test specimen "jumped" out of the tilting bearings when failure occurred.

Figure 3.8. Combined tensile and transverse tension/shear failure at midspan of column S20.

Figure 3.9. Fibre buckling over the entire width of the compression zone of column S23.

A crackling sound indicated coming failure in most cases. Rarely (2 of 27), a localized tensile failure occurred at the tension side of the cross-section, before failure of the whole cross-section. The failure of the cross-section took place suddenly, with a loud bang and consisted of a tensile failure at the tension side of the section and a combined transverse tension/shear failure, which expanded to different extent towards the supports (Figure 3.8). When failing, the column sometimes "jumped" out of the supports due to the released energy (Figure 3.7). The tensile fracture was usually strongly defibrated over a length of up to 80 cm (Figure 3.8). The combined transverse tension/shear failure occurred in several planes (Figure 3.8) and, in the case of stocky columns, sometimes led to a splitting of the cross-section over the entire width and length. In the case of flatwise bending, the failure arose over a longer area; in the case of edgewise bending, the failure was rather punctual and led to a pronounced kink at midspan. For stockier columns, minor fibre buckling occurred at the cross-section corners in the compression zone, along 0.25 to 0.75 of the column length. In some cases, kink bands extended across the entire cross-section width at midspan (Figure 3.9).

4 Numerical simulations

4.1 General

The numerical calculations were executed with a FE model in Abaqus/CAE 2020. The aim was to create a model for analysing in-plane buckling of beech LVL columns and to verify and validate it according to TÖPLER ET AL. (2022) or prEN 1993-1-14 (2022).

4.2 Numerical modelling, model verification and validation

The columns were modelled with measured geometry and material values for validation and nominal geometry and material values in all other cases. At this stage, no imperfections were considered. 20-node quadratic brick elements with a mesh fineness of 50 elements in length, 10 elements in height and 4 elements in width were chosen. For considering a minimum friction coefficient of 0.02 in the tilting bearings according to manufacturer's specifications, a rotational spring was implemented, which generated a comparable moment. An orthotropic material model with linear elastic material properties according to Table 4.1 and a bending / tensile strength of f_m = 100 N/mm² was used.

Table 4.1. Material properties for modelling of beech LVL columns (see KUHLMANN & TÖPLER (2022 a))

E_L [N/mm²]	E_R [N/mm²]	E_T [N/mm²]	G_{LR} [N/mm²]	G_{LT} [N/mm²]	G_{RT} [N/mm²]	ν_{LR} [-]	ν_{LT} [-]	ν_{RT} [-]
16469	840	966	909	1006	50	0.3127	0.5167	0.1978

L = longitudinal, R = radial, T = tangential; 1st index = force direction, 2nd index = deformation direct.

Plasticising in compression was implemented via the von Mises yield criterion, as only longitudinal stresses and strains are of relevant magnitude. An elliptical stress-plastic strain curve according to Figure 3.4 with $f_{c,0,2}$ = 76.9 N/mm², $f_{c,0,1}$ = 0.65 x $f_{c,0,2}$ and $\varepsilon_{pl,0,2}$ = 1.25 x $\varepsilon_{el,0,2}$ was assumed.

Within the verification a sensitivity check and a discretization check according to TÖPLER ET AL. (2022) or prEN 1993-1-14 (2022) were conducted. A detailed report is given by BRÜGEL (2022).

For model validation, a numerical analysis was conducted for each column test considering the measured geometries and moduli of elasticity. The experimental and numerical results were compared. For column S08 the experimentally and numerically determined load-deformation curves are displayed in Figure 3.5. The values agree well, although the numerically determined load-bearing capacities are usually slightly lower (mean 1.6 %, for S08: 3.7 %). This systematic deviation may be due to a too low assumed spring stiffness at the supports in the model.

In the design method *Numerical design with direct resistance check* according to TÖPLER ET AL. (2022) or prEN 1993-1-14 (2022), the reliability of the numerical model (model uncertainty) should be evaluated using the model factor γ_{FE} according to Eq. (1). The experimentally and numerically determined load-bearing capacities R_{test} and R_{check} deviate from each other by a maximum of 5.6 %. The mean value is m_x (R_{test} / R_{check}) = 1.016, the coefficient of variation is V_x (R_{test} / R_{check}) = 0.023 and k_n = 1.76 (EN 1990 (2010)). The model factor can be determined to a very low value of γ_{FE} = 1.026. Characteristic load-bearing capacities R_k can be obtained using numerically computed load-bearing capacities R_{check} with Eq. (2).

$$\gamma_{FE} = \frac{1}{m_x(1 - k_n V_x)} \quad (1)$$

with m_x mean value of the ratio R_{test}/R_{check}

R_{test} measured load-bearing capacity / resistance

R_{check} computed load-bearing capacity / resistance

k_n characteristic fractile factor according to EN 1990 (2010), Annex D, Table D.1 (V_X unknown)

V_x coefficient of variation of the ratio R_{test}/R_{check}

$$R_k = \frac{R_{check}}{\gamma_{FE}} \quad (2)$$

The numerical model could thus be verified and validated and the calculated load-bearing capacities agree very well with experimental results. For the verification based on the design approach *Numerical design with direct resistance check* the partial factor for the material failure is assumed to be kept according to the standards.

4.3 Parameter study, results and evaluation

4.3.1 Input

The parameter study was carried out to investigate the buckling behaviour of beech LVL using the verified and validated numerical model. No load eccentricity was considered, but a sinusoidal bow imperfection e_y. In terms of cross-sectional dimensions, only λ_{rel} significantly affects the buckling behaviour (BRÜGEL (2022)). Therefore, the length is varied between 6 x width and 50 x width, for a fixed width x height = 200 x 200 mm².

In deviation from section 4.2, the following nominal (characteristic) material values according to ETA-14/0354 (2018) were assumed for beech LVL GL75: E_L = 15300 N/mm², $E_R = E_T$ = 400 N/mm² and $G_{LR} = G_{LT}$ = 760 N/mm². Only the results for service class SC1 with $f_{m,k}$ = 75 N/mm² and $f_{c,0,k}$ = 59.4 N/mm² are shown, as the adjustments of the strengths depending on the size effect and service class according to ETA-14/0354 (2018) have no significant influence on the buckling behaviour (BRÜGEL (2022)). To achieve k_c ($\lambda_{rel,0}$ = 0.412) = 1.0, the compressive strength $f_{c,0,k}$ was increased iteratively in the numerical model to the corresponding value $f_{c,0,mod}$ (see discussion of Figure 4.1). This procedure implies that the test specimens, on which the compressive strength $f_{c,0,k}$ was determined, were also imperfect (with e_y = L/1500). Such an assumption is important in terms of mechanical consistency (also for T2O). For determination of $\lambda_{rel,0}$ an Euler buckling mode 2 was assumed.

In the research project DIBt P 52-5- 13.194-2048/19 (KUHLMANN & TÖPLER (2022 b)), imperfection measurements were carried out on 4 buildings with 95 columns and beams made of beech LVL. The mean value of the determined bow imperfections of the col-

umns was $m_x(e_y)$ = L / 3040, the standard deviation $s_x(e_y)$ = L / 5160 and the 95 % quantile value $e_{y,95}$ = L / 1660. Therefore, a bow imperfection of e_y = L / 1500 has been assumed in the parameter study.

Finite element analyses (FEA) with 4 different material models were conducted for GL75: (a) elliptical plastic strains and $f_{c,0,k}$, (b) elliptical plastic strains and $f_{c,0,mod}$, (c) bilinear elasto-plastic material behaviour and $f_{c,0,mod}$, (d) linear elastic material behaviour and $f_{c,0,mod}$.

For comparison with design methods in EN 1995-1-1 (2004) and literature, FE calculations were also performed on glulam GL 24h with nominal (characteristic) material values according to EN 14080 (2013): E_L = 9600 N/mm², $E_R = E_T$ = 250 N/mm², $G_{LR} = G_{LT}$ = 540 N/mm², G_{RT} = 54 N/mm², $f_{m,k}$ = 24 N/mm² and $f_{c,0,k}$ = 24 N/mm². To achieve k_c ($\lambda_{rel,0}$ = 0.331) = 1.0, $f_{c,0,k}$ was increased iteratively in the numerical model to the corresponding value $f_{c,0,mod}$. A bow imperfection of e_y = L/1100 was applied.

FEA with 3 different material models were conducted for GL 24h: (a) elliptical plastic strains ($\varepsilon_{pl,0,2}$ = 0.25 x $\varepsilon_{el,0,2}$ and $f_{c,0,1}$ = 0.75 x $f_{c,0,2}$) and $f_{c,0,mod}$, (b) bilinear elasto-plastic material behaviour and $f_{c,0,mod}$, (c) linear elastic material behaviour and $f_{c,0,mod}$.

Structural imperfections were neglected, since for the independent input variables material parameters and geometric imperfections characteristic and 95 % quantile values were used. It is assumed that these safe-side assumptions cover negative influences of structural imperfections.

4.3.2 Results and discussion

The computed normalised load-bearing capacities k_c of beech LVL GL75 are plotted in Figure 4.1 over the relative slenderness ratio λ_{rel}. The diagram is supplemented with calculation results of ELM with β_c = 0.1, T2O with e_y = L/1500 and the critical buckling load N_{crit}. The shaded area highlights the difference between ELM and FEA with elliptical plasticising. It can be shown that the adjustment $f_{c,0,mod}$ is necessary to obtain accurate results for slenderness $\lambda_{rel,0}$. Nevertheless, the numerically determined load-bearing capacities using a realistic plasticising approach are up to 15 % below the results of calculations with ELM and T2O (see shaded area). The curves of ELM and T2O agree well with numerical results with bilinear or linear elastic material behaviour under compression. The influence of the plastic material behaviour is also illustrated in Figure 3.5 for column S08 where, assuming bilinear material behaviour, 10 % higher load-bearing capacities can be achieved than with the realistic assumption of plasticising according to Figure 3.4. It has to be concluded that the reduction of the stiffness *EI* due to plasticising significantly reduces the load-bearing capacity of medium slender columns (λ_{rel} = 0.4 to 1.3). For GL 24h a slightly less pronounced reduction of the load-bearing capacities from FE analyses can also be observed in comparison with ELM (Figure 4.2).

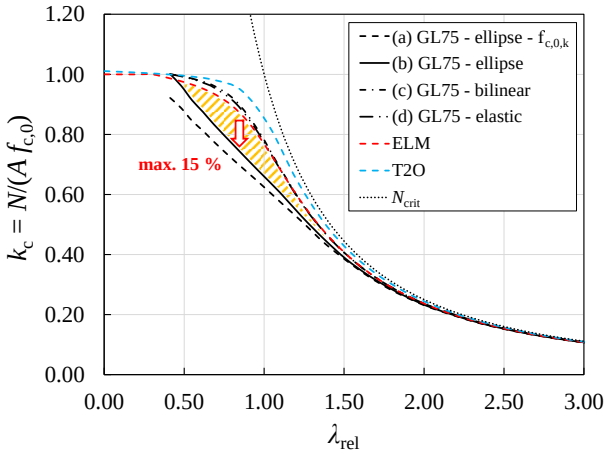

*Figure 4.1. Numerically determined buckling curves of **beech LVL GL75** in comparison with T2O and ELM, the shaded area is the difference between ELM and FEA with elliptical plasticising.*

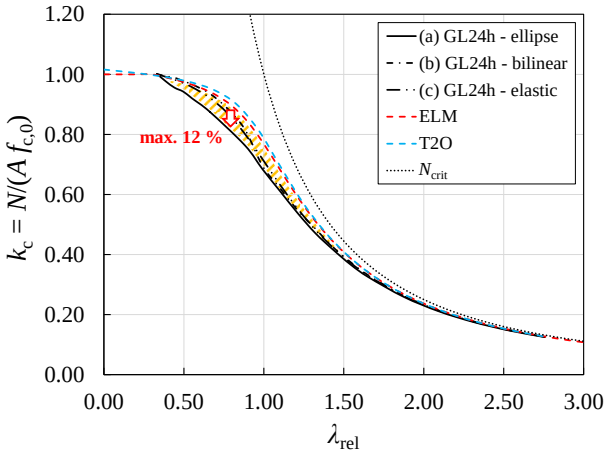

*Figure 4.2. Numerically determined buckling curves of **glulam GL 24h** in comparison with T2O and ELM, the shaded area is the difference between ELM and FEA with elliptical plasticising.*

Possible reasons for the deviations between ELM and FEA are discussed below:

- FE model itself: Since it showed very good agreement with the experimental investigations this reason can be ruled out.
- Input parameters of FEM: β_c in ELM method was derived based on extensive numerical investigations by EHLBECK & BLAß (1987) with scattering input parameters for material (*Karlsruher Rechenmodell*) and bow imperfections using the Monte Carlo method. The characteristic buckling curve was determined from 5 % fractile of the load-bearing capacities. As a simplification, in the FE model presented in this paper characteristic and 95 % quantile values were used for material parameters and geometric imperfections. It is expected, that these two different approaches (full probabilistic with Monte Carlo method vs characteristic input values) may lead to differences. However, differences of up to 12 % can probably not be explained by this.
- Geometrical imperfections: As these are chosen according to EHLBECK & BLAß (1987) for GL 24h, this cannot be the reason.
- Structural imperfections: Their neglect should have a positive impact on the load-bearing capacities from FEA, if any.
- Size effect on tensile / bending strength: As the load-bearing capacity of the presented numerical model was always governed by the peak of the load-deformation curve (Figure 3.5), where tensile stresses were still lower than $f_{m,k}$, this can be ruled out.
- Plasticising – values of assumed stress-strain curve: For the presented comparative calculations of GL 24h the proportionality limit $f_{c,0,1}$ and the plastic strain $\varepsilon_{pl,0,2}$ were chosen according to GLOS (1978) and EHLBECK & BLAß (1987).
- Plasticising – reduction of bending stiffness *EI*: The reduction of the bending stiffness *EI* due to plasticising and the modelling of this behaviour (ellipsoid stress-strain or bilinear stress-strain) plays a decisive role for the column behaviour, see Figure 4.1 and Figure 4.2.

- Models from literature – model uncertainty: In the past, usually strain-based models were used for the investigations of the load-deformation behaviour of timber columns (EHLBECK & BLAß (1987), THEILER (2014), FRANGI ET AL. (2015), EHRHART ET AL. (2019)).
  Results of the strain-based model of THEILER (2014) (see Figure 4.9 in THEILER (2014)) were recalculated with the FE model presented here. Differences of load-bearing capacities were below 2 %. As the strain-based model of THEILER (2014) was, except for negligible simplifications, identical to the one of EHLBECK & BLAß (1987), the different modelling techniques (strain-based and FEA) should not have a significant influence.

From this discussion it is concluded that the deviations of load-bearing capacities between ELM and own numerical calculations for GL 24h (Figure 4.2) are mainly caused by different input parameters (full probabilistic vs characteristic values). For beech LVL GL75 the deviations of ELM and own numerical calculations (Figure 4.1) are additionally increased by the high plastic strains of beech LVL.

5 Design proposal

Based on the safe-side approach considering nominal values for strengths, stiffnesses and bow imperfections and without redefining the partial safety factor in a full probabilistic approach, for the design verification of slender beech LVL columns made of GL75 (ETA-14/0354 (2018)) following adaptions (red) of the effective length method (ELM) in EN 1995-1-1 (2004) may be applied:

$$\frac{\sigma_{c,0,d}}{k_c \, f_{c,0,d}} \leq 1 \tag{3}$$

$$k_c = \frac{1}{k + \sqrt{k^2 - \lambda_{rel}^2}} \tag{4}$$

$$k = 0.5 \left(1 + \beta_c \left(\lambda_{rel} - \lambda_{rel,0}\right) + \lambda_{rel}^2\right) \tag{5}$$

$$\beta_c = k_{pl} \cdot \frac{e_y}{L} \cdot \pi \sqrt{\frac{3 \cdot E_{0,05}}{f_{c,0,k}}} \cdot \frac{f_{c,0,k}}{f_{m,k}} \tag{6}$$

with $\lambda_{rel,0} = 0.4$ critical relative slenderness ratio of beech LVL GL75

$k_{pl} = 6$ factor accounting for the bending stiffness reduction due to plasticising of beech LVL GL75 (empirically derived from FEA)

$e_y / L = 1 / 1500$ bow imperfection of beech LVL GL75

Alternatively, $\beta_c = 0.3$ may be assumed.

The mechanically correct decomposition of β_c based on SCHÄNZLIN (2022) allows to adjust β_c depending on material parameters and bow imperfections. The additional introduction of the factor k_{pl} accounts for the bending stiffness reduction due to plasticising. Thereby, the different effects are clearly separated. Alternatively, similar results are achieved by assuming a value of $\beta_c = 0.3$.

For design verification based on calculations of second order theory (T2O) it is proposed to account for the effects of plasticising on the bending stiffness *EI* by adapting the equivalent bow imperfections $e_{y,equ}$ analogous to Eq. (6):

$$e_{y,equ} = k_{pl} \cdot e_y \tag{7}$$

Results of the adapted design methods ELM with $\beta_c = 0.3$ and T2O in Figure 5.1 show good agreement with the numerically determined characteristic load-bearing capacities of beech LVL columns. It remains to be discussed whether T2O should generally be adapted to account for k_c ($\lambda_{rel,0}$) = 1.0 (see modification of $f_{c,0,k}$ in Figure 4.1). The experimental results are also well represented by the proposed design equations (Figure 5.2). The slight overestimation (5 %) of the load-bearing capacities with the modified ELM occurs in both numerical (Figure 5.1) and experimental results (Figure 5.2) for 0.5 ≤ λ_{rel} ≤ 1.0 due to the shape of the k_c curve.

Creep, load eccentricities and sway imperfections should be considered separately. Application limits of ELM for large external bending moments should be considered.

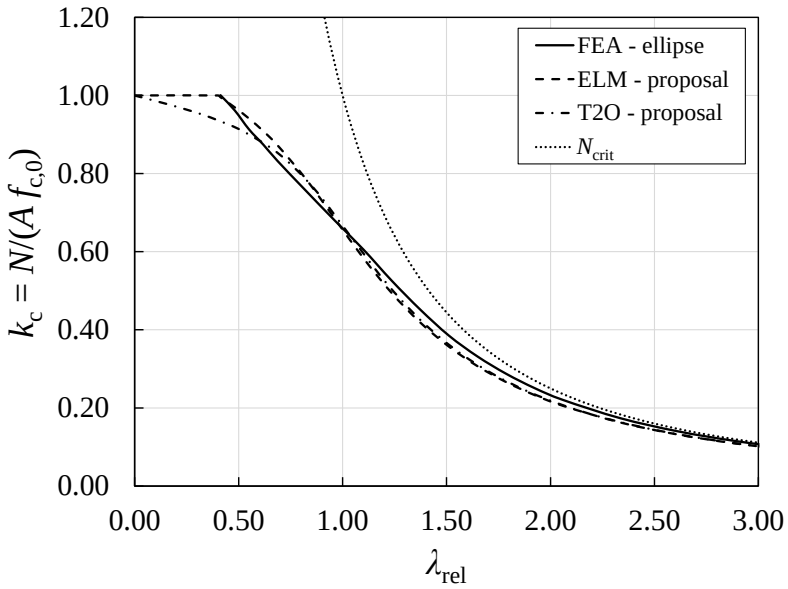

Figure 5.1. Numerically determined buckling curves of beech LVL GL75 in comparison with proposed adapted T2O and ELM.

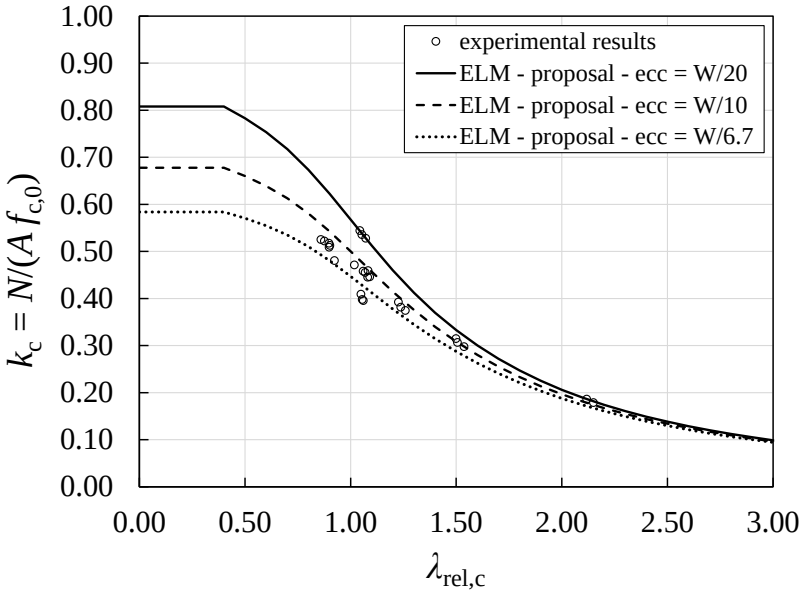

Figure 5.2. Experimentally determined, normalised load-bearing capacities k_c in comparison with proposed adapted ELM.

6 Summary and outlook

This paper aims to study the in-plane buckling behaviour of columns made of beech LVL GL75 (ETA-14/0354 (2018)) with extensive experimental and numerical investigations.

Results of 27 buckling tests on full size timber columns and preceding tests to determine the bending modulus of elasticity and the stress-strain behaviour under compression parallel to the grain are described. The experimentally determined normalised load-bearing capacities k_c of the columns show only minor scattering and follow well the expected shape of a buckling curve (Figure 3.6 and Figure 5.2). All columns experience large horizontal deformations (> 60 mm) before failure. The maximum load-bearing capacity was not determined by the first point of partial failure, but by the peak of the load-deformation curve (Figure 3.5). From the preceding compression tests, it is concluded, that plasticising before reaching the compressive strength $f_{c,0,2}$ has a significant influence and should be considered for beech LVL GL75. The mean value of the proportionality limit (beginning of plasticising) for compression parallel to the grain was observed at 65 % of the compression strength ($f_{c,0,1} \approx 0.65 \times f_{c,0,2}$) and plastic strains of 4 to 6.5 times the elastic strains ($\varepsilon_{pl,0,2} \approx 1.25 \times \varepsilon_{el,0,2}$) occurred when the compression strength $f_{c,0,2}$ was reached.

A numerical model for analysing the in-plane buckling behaviour of beech LVL columns was developed, verified and validated by the experimental results according to TÖPLER ET AL. (2022) or prEN 1993-1-14 (2022). The mean and maximum deviations of experimental and numerical load-bearing capacities were 1.6 % and 5.6 %.

Based on measurements on columns and beams made of beech LVL, a bow imperfection of e_y = L / 1500 was included in the numerical calculations.

The numerical calculations revealed that the load-bearing capacity of medium slender beech LVL columns is up to 15 % smaller compared to the current verifications according to ELM, which is to a large extend due to plasticising reducing the bending stiffness *EI*.

Based on the experimental and numerical investigations, an adjustment of β_c = 0.3 and $\lambda_{rel,0}$ = 0.4 is recommended for the design of columns made of beech LVL GL75 using the effective length method (ELM). For calculations according to second order theory (T2O) an adaption of the equivalent bow imperfection $e_{y,equ} = k_{pl} \times e_y$ is proposed (with e_y = L / 1500 and k_{pl} = 6 for beech LVL to account for a reduced bending stiffness *EI* due to plasticising).

Future investigations on the effects of statistical scattering in form of a reliability analysis may allow for further modifications.

7 Acknowledgements

The research was supported by the Deutsche Forschungsgemeinschaft (DFG, German Research Foundation) under Germany´s Excellence Strategy – EXC 2120/1 – 390831618. The research project (P 52-5- 13.194-2048/19) was supervised by Deutsches Institut für Bautechnik (DIBt) and carried out with financial support from the Federal States. These supports are gratefully acknowledged.

We thank the Material Testing Institute (MPA) of the University of Stuttgart, Department Building Construction and Component Testing and the Department Timber Constructions for their support.

We thank Pollmeier Massivholz GmbH & Co. KG for the provision of the test specimens.

Many thanks to Andrea Frangi, Thomas Ehrhart and Stephan Schilling from ETH Zürich for sharing their tests results and experiences from the research project WHFF-CH 2020.11.

We thank Heni Architekten, Implenia Schweiz AG and Pollmeier Massivholz GmbH & Co. KG (in alphabetical order) for allowing measurements of the assembly tolerances on selected timber buildings.

Many thanks to the Institute for Photogrammetry (ifp) of the University of Stuttgart and especially to Lena Joachim and Edward Necşulescu for carrying out the laser scanning and advising on the measurements' evaluation.

8 References

Buchanan, A. H.; Johns, K. C.; Madsen, B. (1985): Column Design Methods for Timber Engineering. CIB-W18, 18-2-1, Beit Oren, Israel.

Brügel, F. (2022): Experimentelle und numerische Untersuchung des Tragverhaltens von Buchen LVL (in German). Master thesis, Institute for Structural Design, University of Stuttgart, Germany.

Dill-Langer, G. (2014): Tragfähigkeit und Baupotenziale von Buchen-Furnierschichtholz (in German). In: Internationales Holzbau Forum (IHF), Garmisch, Germany.

DIN 4074 (1958): Blatt 1 – Bauholz für Holzbauteile – Gütebedingungen für Bauschnittholz (Nadelholz) (in German). German Institute of Standardization (DIN), Berlin.

Ehlbeck, J.; Blaß, H. J. (1987): Zuverlässigkeit von Holzdruckstäben (in German). Research report, University Fridericiana Karlsruhe, Germany.

Ehrhart, T.; Steiger, R.; Frangi, A. (2021 a): Influence of the moisture content on the compressive strength and modulus of elasticity parallel to the grain of engineered hardwood products (EHP). In: Proceedings of the 8th meeting of International Network on Timber Engineering Research (INTER), 54-12-2, online, 2021.

Ehrhart, T.; Steiger, R.; Frangi, A.; Strahm, T.; Bernasconi, A. (2021 b): Laubholzstützen - Druckfestigkeit und E-Modul parallel zur Faserrichtung und Einfluss der Holzfeuchte (in German). Research report, WHFF-CH 2020.11, ETH Zürich, Switzerland.

Ehrhart, T.; Steiger, R.; Palma, P.; Gehri, E.; Frangi, A. (2019): Compressive strength and buckling resistance of GLT columns made of European beech (Fagus sylvatica L.). In: Proceedings of the 6th meeting of International Network on Timber Engineering Research (INTER), 52-12-1, Tacoma, USA.

EN 408 (2010): Structural Timber and Glued Laminated Timber – Determination of Some Physical and Mechanical Properties. European Committee for Standardization (CEN), Brussels, Belgium, with corrections and amendments + A1:2012.

EN 1990 (2010): Eurocode 0: Basis of structural design. European Committee for Standardization (CEN), Brussels, Belgium, with corrections and amendments + A1:2005 and AC:2010.

EN 1995-1-1 (2004): Eurocode 5: Design of timber structures – Part 1-1: General – Common rules and rules for buildings. European Committee for Standardization (CEN), Brussels, with corrections and amendments + AC:2006 and A1:2008.

EN 14080 (2013): Timber structures - Glued laminated timber and glued solid timber - Requirements. European Committee for Standardization (CEN), Brussels.

ETA-14/0354 (2018): Beam BauBuche GL75. Austria Institute of Construction Engineering (OIB), Vienna, Austria.

Frangi, A.; Steiger, R.; Theiler, M. (2015): Design of timber members subjected to axial compression or combined axial compression and bending based on 2nd order the-

ory. In: Proceedings of the 2nd meeting of International Network on Timber Engineering Research (INTER), 48-2-2, Šibenik, Croatia.

Glos, P. (1978): Zur Bestimmung des Festigkeitsverhaltens von Brettschichtholz bei Druckbeanspruchung aus Werkstoff- und Einwirkungskenngrößen (in German). Dissertation, Technical University of Munich, Germany.

Grosse, M. (2005): Zur numerischen Simulation des physikalisch nichtlinearen Kurzzeittragverhaltens von Nadelholz am Beispiel von Holz-Beton-Verbundkonstruktionen (in German). Dissertation. Bauhaus-Universität Weimar, Germany.

Kuhlmann, U.; Töpler, J.; Gauß, J.; Buchholz, L. (2022): Integrated approach of testing and numerical verifications (IATN). Research project RP 7, DFG Cluster of Excellence "Integrative Computational Design and Construction for Architecture", EXC 2120/1 – 390831618, Institute of Structural Design, University of Stuttgart, Germany.

Kuhlmann, U.; Töpler, J. (2022 a): Experimentelle und numerische Untersuchungen von Brettschichtholz aus Buchen-Furnierschichtholz (BauBuche) (in German). In: Doktorandenkolloquium Holzbau Forschung und Praxis. online.

Kuhlmann, U.; Töpler, J. (2022 b): Imperfektionsmessungen an stabilitätsgefährdeten Holzbauteilen - Schlussbericht (in German). Research report, DIBt P 52-5- 13.194-2048/19, Institute of Structural Design, University of Stuttgart, Germany.

prEN 1993-1-14 (15 February 2022): Eurocode 3: Design of steel structures – Part 1-14: Design assisted by finite element analysis (draft version). CEN/TC 250/SC 3/WG 22 N 55.

prEN 1995-1-1 (28 October 2021): Eurocode 5: Design of timber structures – Common rules and rules for buildings – Part 1-1: General (Consolidated draft for informal inquiry). CEN/TC 250/SC 5 N 1488.

Schänzlin, J. (10 February 2022): kc-method – consideration of creep deformations. CEN/TC 250/SC 5/WG 3 N 354.

Theiler, M. (2014): Stabilität von axial auf Druck beanspruchten Bauteilen aus Vollholz und Brettschichtholz (in German). Dissertation. ETH Zürich, Switzerland.

Töpler, J.; Buchholz, L.; Machanek, S.; Kuhlmann, U. (2022): Guidelines for a Finite Element Based Design of Timber Structures (unpublished). Institute for Structural Design, University of Stuttgart, Germany.